Effects of Charge State and Cationizing Agent on the Electron Capture Dissociation of a Peptide

Anthony T. Iavarone, Kolja Paech, and Evan R. Williams*

Department of Chemistry, University of California, Berkeley, California 94720-1460

Electron capture dissociation (ECD) is a promising method for de novo sequencing proteins and peptides and for locating the positions of labile posttranslational modifications and binding sites of noncovalently bound species. We report the ECD of a synthetic peptide containing 10 alanine residues and 6 lysine residues uniformly distributed across the sequence. ECD of the $(M + 2H)^{2+}$ produces a limited range of c (c_7-c_{15}) and z (z_9-z_{15}) fragment ions, but ECD of higher charge states produces a wider range of c (c_2-c_{15}) and z (z_2-z_6, z_9-z_{15}) ions. Fragmentation efficiency increases with increasing precursor charge state, and efficiencies up to 88% are achieved. Heating the $(M + 2H)^{2+}$ to 150 °C does not increase the observed range of ECD fragment ions, indicating that the limited products are due to backbone cleavages occurring near charges and not due to effects of tertiary structure. ECD of the $(M + 2Li)^{2+}$ and $(M + 2Cs)^{2+}$ produces di- and monometalated analogues of the same c and z ions observed from the $(M + 2H)^{2+}$, with the abundance of dimetalated fragment ions increasing with fragment ion mass, a result consistent with the metal cations being located near the peptide termini to minimize Coulombic repulsion. In stark contrast to the ECD results, collisional activation of cesiated dications overwhelmingly results in ejection of Cs^+. The abundance of cesiated fragment ions formed from ECD of the $(M + Cs + Li)^{2+}$ exceeds that of lithiated fragment ions by 10:1. ECD of the $(M + H + Li)^{2+}$ results in *exclusively lithiated* c and z ions, indicating an overwhelming preference for neutralization and cleavage at protonated sites over metalated sites. These results are consistent with preferential neutralization of the cation with the highest recombination energy.

Although mass spectrometry (MS) and tandem mass spectrometry (MS/MS) have been used to characterize peptides for more than three decades,[1,2] the developments of electrospray ionization (ESI)[3] and matrix-assisted laser desorption/ionization[4] have dramatically expanded the size and type of molecules amenable to characterization by MS/MS. For example, ESI has been used to form intact gas-phase ions from virus particles (4.0×10^7 Da)[5] and DNA molecules as large as 1.2×10^8 Da.[6] ESI-MS and ESI-MS/MS experiments can be performed using as little as 10^{-18} mol of sample.[7] For these measurements, Fourier transform (FT) MS has the advantages of ultrahigh resolution, multichannel detection, and MS^n capabilities.[8,9] Dissociation methods in FTMS, including collisionally activated dissociation (CAD),[10] surface-induced dissociation,[11,12] infrared multiphoton dissociation,[13] and blackbody infrared radiative dissociation,[14,15] have been used to obtain sequence information and locations of posttranslational modifications (PTMs) in biomolecules. With these activation methods, the most labile bonds within an ion are typically cleaved. This often produces incomplete sequence coverage, the loss of PTMs, and a lack of backbone cleavages within regions enclosed by disulfide bridges.

The recently developed method of electron capture dissociation (ECD),[16−25] pioneered by McLafferty,[16] produces greater sequence information from protein and peptide ions than other activation

* Corresponding author. E-mail: williams@cchem.berkeley.edu. Fax: (510) 642-7714.

(1) Agarwal, K. L.; Johnstone, R. A.; Kenner, G. W.; Millington, D. S.; Sheppard, R. C. *Nature* **1968**, *219*, 498−499.
(2) McLafferty, F. W.; Venkataraghavan, R.; Irving, P. *Biochem. Biophys. Res. Commun.* **1970**, *39*, 274−278.
(3) Fenn, J. B.; Mann, M.; Meng, C. K.; Wong, S. F.; Whitehouse, C. M. *Science* **1989**, *246*, 64−71.
(4) Hillenkamp, F.; Karas, M.; Beavis, R. C.; Chait, B. T. *Anal. Chem.* **1991**, *63*, 1193A−1202A.
(5) Siuzdak, G.; Bothner, B.; Yeager, M.; Brugidou, C.; Fauquet, C. M.; Hoey, K.; Chang, C. M. *Chem. Biol.* **1996**, *3*, 45−48.
(6) Chen, R.; Cheng, X.; Mitchell, D. W.; Hofstadler, S. A.; Wu, Q.; Rockwood, A. L.; Sherman, M. G.; Smith, R. D. *Anal. Chem.* **1995**, *67*, 1159−1163.
(7) Valaskovic, G. A.; Kelleher, N. L.; McLafferty, F. W. *Science* **1996**, *273*, 1199−1202.
(8) Marshall, A. G. *Int. J. Mass Spectrom.* **2000**, *200*, 331−356 and references therein.
(9) Williams, E. R. *Anal. Chem.* **1998**, *70*, 179A−185A.
(10) Senko, M. W.; Speir, J. P.; McLafferty, F. W. *Anal. Chem.* **1994**, *66*, 2801−2808.
(11) Chorush, R. A.; Little, D. P.; Beu, S. C.; Wood, T. D.; McLafferty, F. W. *Anal. Chem.* **1995**, *67*, 1042−1046.
(12) Tsaprailis, G.; Nair, H.; Somogyi, A.; Wysocki, V. H.; Zhong, W. Q.; Futrell, J. H.; Summerfield, S. G.; Gaskell, S. J. *J. Am. Chem. Soc.* **1999**, *121*, 5142−5154.
(13) Little, D. P.; Speir, J. P.; Senko, M. W.; O'Connor, P. B.; McLafferty, F. W. *Anal. Chem.* **1994**, *66*, 2809−2815.
(14) Dunbar, R. C.; McMahon, T. B. *Science* **1998**, *279*, 194−197.
(15) Price, W. D.; Schnier, P. D.; Williams, E. R. *Anal. Chem.* **1996**, *68*, 859−866.
(16) Zubarev, R. A.; Kelleher, N. L.; McLafferty, F. W. *J. Am. Chem. Soc.* **1998**, *120*, 3265−3266.
(17) Kruger, N. A.; Zubarev, R. A.; Horn, D. M.; McLafferty, F. W. *Int. J. Mass Spectrom.* **1999**, *187*, 787−793.
(18) Kelleher, N. L.; Zubarev, R. A.; Bush, K.; Furie, B.; Furie, B. C.; McLafferty, F. W.; Walsh, C. T. *Anal. Chem.* **1999**, *71*, 4250−4253.
(19) Haselmann, K. F.; Jørgensen, T. J. D.; Budnik, B. A.; Jensen, F.; Zubarev, R. A. *Rapid Commun. Mass Spectrom.* **2002**, *16*, 2260−2265.
(20) Breuker, K.; Oh, H.; Horn, D. M.; Cerda, B. A.; McLafferty, F. W. *J. Am. Chem. Soc.* **2002**, *124*, 6407−6420.
(21) Zubarev, R. A.; Haselmann, K. F.; Budnik, B.; Kjeldsen, F.; Jensen, F. *Eur. J. Mass Spectrom.* **2002**, *8*, 337−349.

10.1021/ac035431p CCC: $27.50
Published on Web 00/00/0000

methods. For example, ECD of the 11+ charge state of ubiquitin gave roughly 3 times the sequence information produced by CAD of this same charge state.[16] For five peptides ranging in size from 12 to 17 amino acid residues, Kruger et al. obtained 82−100% sequence coverage by ECD but only 29−69% by CAD.[17] Another advantage of ECD is that $N-C_\alpha$ bonds and disulfide bonds are cleaved while more labile bonds are often left intact. This is useful for localizing labile PTMs to specific amino acid residues. For example, Kelleher et al. performed CAD and ECD on 28-residue peptide ions containing γ-carboxylation on residues 24 and 25.[18] The y and b fragment ions produced by CAD did not retain the γ-CO_2, but ECD produced c ions that retained the γ-CO_2 groups to >90%.[18]

Noncovalent inter- and intramolecular interactions are also left intact during ECD. For example, Haselmann et al. fragmented the 3+ ions of noncovalent homodimers of a 13-mer peptide by CAD and ECD.[19] While CAD resulted in 100% dissociation of the dimer into monomers, ECD of the dimer produced $(M + c_5 + H)^+$, $(M + c_6 + H)^+$, and $(M + c_8 + H)^+$, products of backbone bond cleavage with the preservation of noncovalent intermolecular interactions.[19] The number of backbone cleavages observed from ECD of 6+ ions of ubiquitin increases from 9 to 36 as the ion cell temperature is increased from 25 to 155 °C.[20] The increased sequence coverage at higher temperatures is attributed to the heat-induced unfolding of the tertiary structure of the gas-phase ions. Similarly, increasing the charge state of the precursor ion increases the sequence coverage obtained by ECD at 25 °C. For example, the number of observed backbone cleavages for ubiquitin increases from 0 to 50 as the precursor charge state is increased from 5+ to 13+. Heating the 13+ charge state of ubiquitin to 125 °C does not change the ECD spectrum, indicating that no significant tertiary structure remains in these highly charged ions at ambient temperature.[20]

The detailed mechanism of ECD is the subject of active investigation, and progress in this area has been recently reviewed.[21] McLafferty proposed that capture of an electron generates a high-*n* Rydberg state, which can undergo an avoided crossing to a repulsive surface, followed by dissociation.[22,23] Alternatively, capture of an electron by a peptide or protein ion, with subsequent electron transfer, can result in the formation of a hypervalent species.[16,22] For example, electron capture at a protonated lysine residue solvated by a nearby carbonyl oxygen, $R-NH_2\cdots H^+\cdots O{=}C(R')NHR''$, generates the hypervalent species $R-NH_2\cdots H^+\cdots O{=}C(R')NHR''$. Addition of the hydrogen atom to the carbonyl oxygen instead of the amine is favored by ∼2 eV.[16] Subsequent dissociation of the $N-C_\alpha$ bond forms c and z product ions. McLafferty suggested that formation of c and z ions can be very fast and that this process is nonergodic.[16] However, density functional and Møller−Plesset perturbational calculations on model peptide and amide radicals performed by Turecek indicate that the dissociation of the $N-C_\alpha$ bond is fast (unimolecular rate constants $>10^5$ s^{-1}) for gas-phase radicals and cation−radicals that have been thermalized at 298 K, consistent with an ergodic process.[24] Interestingly, disulfide bridges have a high propensity to be cleaved in ECD. Disulfide bridges are not expected to be charged because the proton affinity of an −S−S− group is 24 kcal/mol lower than that of an amide carbonyl.[22] McLafferty and coworkers proposed that the high propensity for disulfide cleavage is due to the hydrogen atom exploring the molecule before being captured and inducing dissociation at a site of high hydrogen atom affinity (The hydrogen atom affinity of an −S−S− group is 24 kcal/mol higher than that of an amide carbonyl).[22]

Hudgins et al. performed ECD on peptides cationized with Na^+ or K^+ instead of H^+, and on peptides with permanent charges, i.e., lysine residues functionalized with quaternary ammonium groups ($-N(CH_3)_3^+$). ECD of these species produced the alkalated and fixed-charge analogues of the c and z ions formed from the protonated peptides. The authors proposed that $N-C_\alpha$ bonds are cleaved by direct dissociative electron attachment.[25]

Here, we examine the effects of precursor ion charge state and cationizing agent on the ECD of a synthetic 16-residue peptide containing only alanine and lysine residues. This peptide was selected for this study to minimize any effects associated with different amino acid residues, while making available a wide range of charge states. The N-terminus is acetylated, and the C-terminus is amidated. The lack of acidic hydrogens prevents salt bridge formation.

EXPERIMENTAL SECTION

Instrument. Experiments are performed on a Fourier transform mass spectrometer equipped with a 9.4-T superconducting magnet and an external ESI source. This instrument is described elsewhere.[26] Ions are formed using electrospray ionization either by nanoelectrospray[27] or by infusing solution at a flow rate of 1.0 μL/min using a syringe pump (Harvard Apparatus, South Natick, MA) and a metal capillary. For the latter, the electrospray voltage is 4.4 kV, and pneumatic assistance is used. For nanoelectrospray, needles are made from 1.0-mm-o.d./0.78-mm-i.d. borosilicate capillaries. These capillaries are pulled to a tip with an inner diameter of ∼4 μm using a Flaming/Brown micropipet puller (model P-87, Sutter Instruments, Novato, CA). The electrospray is initiated by applying a potential of ∼800−1200 V to a Pt wire (0.127-mm diameter, Aldrich, Milwaukee, WI) inserted into the nanoelectrospray needle to within ∼2 mm of the tip. The wire and nanoelectrospray needle are held in place with a patch clamp holder (WPI Instruments, Sarasota, FL). The flow rate is between 50 and 200 nL/min. No pneumatic assistance or back pressure is used. The ions and droplets are sampled from atmospheric pressure through a glass capillary. A countercurrent flow of heated nitrogen (120 °C) is used to promote evaporation of the electrospray droplets. Ions are accumulated in an external hexapole ion trap and gated into the cell. Ion trapping and thermalization are enhanced by using nitrogen pulsed into the cell at a peak pressure of $\sim(1-5) \times 10^{-7}$ Torr. The ion of interest is isolated using correlated sweeps.

(22) Zubarev, R. A.; Kruger, N. A.; Fridriksson, E. K.; Lewis, M. A.; Horn, D. M.; Carpenter, B. K.; McLafferty, F. W. *J. Am. Chem. Soc.* **1999**, *121*, 2857−2862.
(23) Zubarev, R. A.; Horn, D. M.; Fridriksson, E. K.; Kelleher, N. L.; Kruger, N. A.; Lewis, M. A.; Carpenter, B. K.; McLafferty, F. W. *Anal. Chem.* **2000**, *72*, 563−573.
(24) Turecek, F. *J. Am. Chem. Soc.* **2003**, *125*, 5954−5963.
(25) Hudgins, R. R.; Håkansson, K.; Quinn, J. P.; Hendrickson, C. L.; Marshall, A. G. *Proceedings of the 50th Annual Conference on Mass Spectrometry and Allied Topics*; Orlando, FL, June 2002.
(26) Jurchen, J. C.; Williams, E. R. *J. Am. Chem. Soc.* **2003**, *125*, 2817−2826.
(27) Wilm, M.; Mann, M. *Anal. Chem.* **1996**, *68*, 1−8.

ECD and CAD. To perform ECD on the isolated ion, electrons are emitted from an indirectly heated dispenser cathode[28] (model STD200, Heatwave Labs, Watsonville, CA) located ~7 cm from the rear trapping plate of the ion cell. The cathode is heated with 1.0−1.2 A and ~5 V. The cathode is biased at −0.1 V during electron injection and at +16 V at all other times. A single electron injection pulse of 0.5−5.0 s is used. A grid of copper wires biased at +10 V and located ~1 cm from the dispenser cathode is used to establish a uniform accelerating field for the electrons. The electrons enter the cell through a 6-mm-diameter hole in the center of the rear trapping plate.

To perform sustained off-resonance irradiation collisionally activated dissociation (SORI-CAD)[29] on the isolated ion, a single-frequency excitation waveform with an applied peak-to-peak potential of 3−12 V and a frequency 1000 Hz below the ion's cyclotron frequency is applied for 0.1−0.5 s. Nitrogen is used as the collision gas and is introduced via a pulsed valve (open for 10−100 ms) to a peak pressure of ~$(1-5) \times 10^{-7}$ Torr. The pressure in the cell returns to ~$(1-5) \times 10^{-9}$ Torr prior to detection. Cell pressures are monitored using an uncalibrated ion gauge located above one of the turbomolecular pumps. A copper jacket is used to heat trapped ions with blackbody radiation, as described previously.[26] The temperature is regulated using a thermocouple interfaced with a digital temperature controller (Omega Engineering, Stamford, CT).

Solutions. Methanol (99.99%) was obtained from EM Science (Gibbstown, NJ). Glacial acetic acid (99.9%) was obtained from Fisher Scientific (Fair Lawn, NJ). Lithium hydroxide (98+%) and *m*-nitrobenzyl alcohol (*m*-NBA; 98%) were obtained from Aldrich Chemical Co. (Milwaukee, WI). Cesium bromide (99.95%) was obtained from Gallard-Schlesinger (Carle Place, NY). The peptide AcHN-$(AKAAK)_3$A-NH_2 (6KI; MW 1538)[30] was synthesized by Dr. David King (UC Berkeley) and is used without further purification. For all experiments except those involving $(M + Cs + Li)^{2+}$, the electrospray solution is 47% water/50% methanol/3% acetic acid, the peptide concentration is 10^{-5} M, and regular electrospray is used. To form $(M + 2Li)^{2+}$, $(M + 2Cs)^{2+}$, and $(M + H + Li)^{2+}$, lithium hydroxide, cesium bromide, and lithium hydroxide are added to the electrospray solutions at concentrations of 3, 5, and 0.2 mM, respectively. To form $(M + Cs + Li)^{2+}$, lithium hydroxide and cesium bromide are both added, at 2 mM, to a 90% water/10% methanol solution containing the peptide at 5×10^{-5} M. To promote the formation of higher charge states, *m*-NBA is added to the electrospray solutions at a level of 0.5%.[31−33] All solution compositions are reported on a volume/volume basis. The average charge state is calculated as described previously.[31] To assess the reproducibility of ECD spectra, ECD of the $(M + 2H)^{2+}$ of 6KI was performed three times on different days within a one-week period under the same set of conditions. Errors are reported as ± one standard deviation from the mean for three replicate experiments. The fragmentation efficiency is defined as the ratio of the summed abundances of the fragment ions, i.e., all ions appearing in the spectrum except for the residual precursor and the reduced undissociated precursor ions, to the total ion abundance in the ECD mass spectrum.

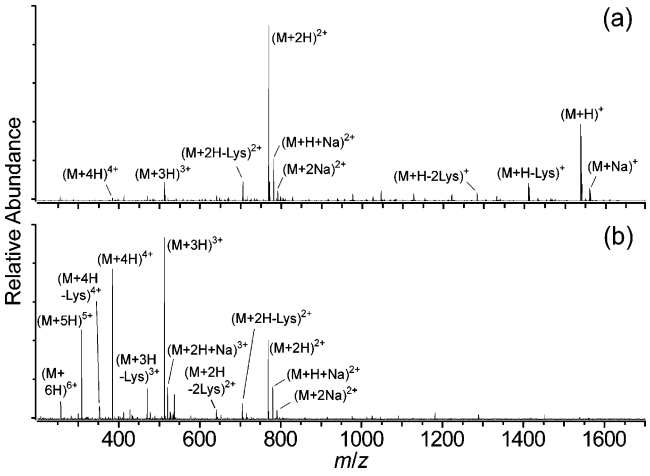

Figure 1. ESI mass spectra of 6KI (10^{-5} M) formed from 47% water/50% methanol/3% acetic acid with (a) 0 and (b) 0.5% *m*-nitrobenzyl alcohol. The capillary exit voltage, second skimmer voltage, and hexapole offset for (a) and (b) are 150 and 100, 8.0 and 9.0, and 5.0 and 4.0 V, respectively. Peaks due to impurities in the sample, e.g., 6KI lacking one or two lysine residues, and peaks arising from sodium adduction are present in the mass spectra (the sample was not purified after synthesis).

RESULTS AND DISCUSSION

Electrospray Charge Distributions. The solution composition and instrument conditions are adjusted to maximize the abundance of the precursor charge state of interest. For example, low charge states of 6KI (10^{-5} M) are enhanced by electrospraying from 47% water/50% methanol/3% acetic acid solutions with a capillary exit voltage of 150 V, a second skimmer voltage of 8.0 V, and a hexapole offset of 5.0 V (Figure 1a). The $(M + H)^+$, $(M + 2H)^{2+}$, $(M + 3H)^{3+}$, and $(M + 4H)^{4+}$ are formed at 44, 100, 12, and 3% relative abundance, respectively, and the average charge state is 1.8. Adding *m*-NBA at a level of 0.5% to the solution and adjusting the capillary exit voltage to 100 V, the second skimmer voltage to 9.0 V, and the hexapole offset to 4.0 V produces the $(M + 2H)^{2+}$, $(M + 3H)^{3+}$, $(M + 4H)^{4+}$, $(M + 5H)^{5+}$, and $(M + 6H)^{6+}$ at relative abundances of 44, 100, 82, 50, and 10%, respectively, resulting in an average charge state of 3.6 (Figure 1b). The $(M + 6H)^{6+}$ corresponds to protonation of all six lysine residues. The other instrument conditions for the spectra in Figure 1 are the same.

Electron Capture Dissociation of Protonated Ions. Charge states of 6KI between $(M + 2H)^{2+}$ and $(M + 5H)^{5+}$ were fragmented by ECD (Figures 2 and 3). For ECD of the $(M + 2H)^{2+}$ (Figure 2a), the base peak is the residual precursor ion, which is 41 ± 12% of the total ion abundance (TIA). Also observed are the reduced (singly charged) precursor ion and the reduced precursor ion that has lost 58 Da (presumably loss of the N-terminal acetate group, C_2H_4NO), at 4.4 ± 2.0 and 4.8 ± 1.5% TIA, respectively. The predominant fragment ions resulting from single backbone cleavages are c- (c_7-c_{15}) and z- (z_9-z_{15}) series

(28) Tsybin, Y. O.; Håkansson, P.; Budnik, B. A.; Haselmann, K. F.; Kjeldsen, F.; Gorshkov, M.; Zubarev, R. A. *Rapid Commun. Mass Spectrom.* **2001**, *15*, 1849−1854.
(29) Gauthier, J. W.; Trautman, T. R.; Jacobson, D. B. *Anal. Chim. Acta* **1991**, *246*, 211−225.
(30) Marqusee, S.; Robbins, V. H.; Baldwin, R. L. *Proc. Natl. Acad. Sci. U.S.A.* **1989**, *86*, 5286−5290.
(31) Iavarone, A. T.; Jurchen, J. C.; Williams, E. R. *Anal. Chem.* **2001**, *73*, 1455−1460.
(32) Iavarone, A. T.; Williams, E. R. *Int. J. Mass Spectrom.* **2002**, *219*, 63−72.
(33) Iavarone, A. T.; Williams, E. R. *J. Am. Chem. Soc.* **2003**, *125*, 2319−2327.

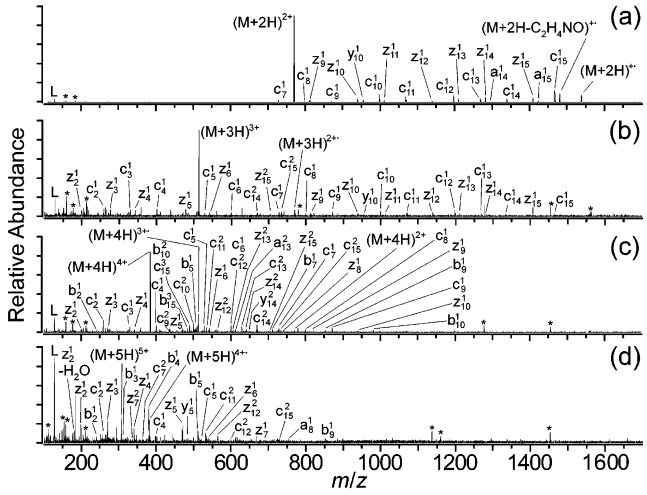

Figure 2. ECD spectra of the (a) $(M + 2H)^{2+}$, (b) $(M + 3H)^{3+}$, (c) $(M + 4H)^{4+}$, and (d) $(M + 5H)^{5+}$ of 6KI. The "L" denotes $C_6H_{13}N_2O^+$ (*m*/*z* 129), presumably a product of internal cleavage and rearrangement of a lysine residue. Noise peaks are indicated by asterisks.

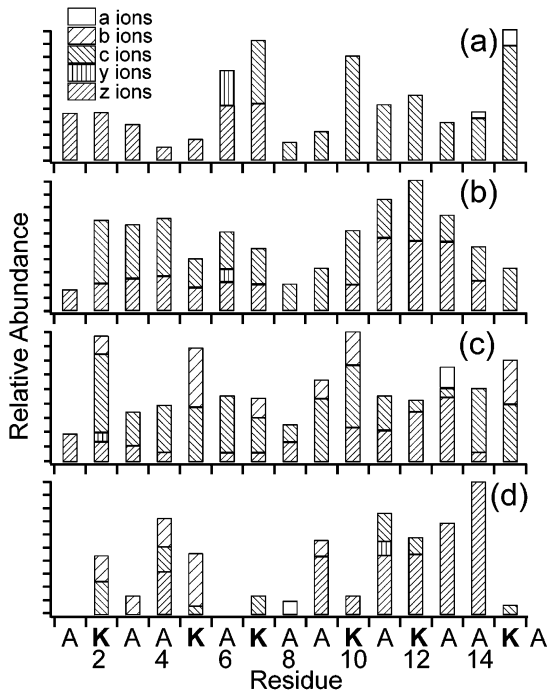

Figure 3. ECD fragment ion plots of the (a) $(M + 2H)^{2+}$, (b) $(M + 3H)^{3+}$, (c) $(M + 4H)^{4+}$, and (d) $(M + 5H)^{5+}$ of 6KI.

ions, collectively comprising 29 ± 3 and 15 ± 3% TIA, respectively. Observed at lower abundance are a-series ions (a_{14} and a_{15}) and y_{10}, comprising 1.3 ± 0.5 and 2.0 ± 0.3% TIA, respectively. $C_6H_{13}N_2O^+$ (*m*/*z* 129), a fragment ion presumably resulting from internal cleavage and rearrangement of a lysine residue, is observed at 2.3 ± 1.6% TIA.

ECD of the next highest charge state, $(M + 3H)^{3+}$, results in a significantly wider range of c and z ions to include c_2-c_6 and z_2-z_6, as well as b_{15}, y_{10}, and $C_6H_{13}N_2O^+$, observed at 1.2, 0.7, and 6.9% TIA, respectively (Figures 2b and 3b). ECD of the $(M + 4H)^{4+}$ results in several b ions (the b ions have the same masses as the corresponding c ions that have lost NH_3), comprising 11% TIA, in addition to the same range of c and z ions observed from the $(M + 3H)^{3+}$, with the addition of z_8 and the omission of z_{11}

Table 1. ECD Fragmentation Efficiencies of Charge States of 6KI

precursor ion	fragmentation efficiency (%)	fragmentation efficiency without $C_6H_{13}N_2O^+$ (%)[a]	residual precursor (%)[b]	theoretical residual precursor (%)[c]
$(M + 2H)^{2+}$	54 ± 10[d]	52 ± 8[d]	41 ± 12[d]	
$(M + 3H)^{3+}$	64	57	33	18
$(M + 4H)^{4+}$	69	63	24	10
$(M + 5H)^{5+}$	88	62	10	7

[a] The fragmentation efficiency calculated without including the internal cleavage product $C_6H_{13}N_2O^+$ (*m*/*z* 129). [b] The experimentally observed abundance of the residual precursor ion, relative to the total ion abundance of the spectrum. [c] The theoretical residual precursor ion abundance, normalized to the experimentally observed value for the $(M + 2H)^{2+}$ (41%). Based on the quadratic dependence of the electron capture cross section on charge state (ref 23). [d] Errors are ± one standard deviation from the mean for three replicate experiments, as described in the Experimental Section.

(Figures 2c and 3c). $C_6H_{13}N_2O^+$ is observed at 5.4% TIA. For the $(M + 5H)^{5+}$, ECD results in a 5-fold increase in the relative abundance of $C_6H_{13}N_2O^+$ and a shift toward lower mass fragment ions compared to that obtained from the $(M + 4H)^{4+}$ (Figures 2d and 3d). For example, the combined abundance of c_2-c_7, z_2-z_7, and b_2-b_5 increases from 48 to 80% of fragment ions not including $C_6H_{13}N_2O^+$, as the precursor charge state is increased from $(M + 4H)^{4+}$ to $(M + 5H)^{5+}$. The average masses of c ions, weighted by ion abundance, formed from the 2+ to 5+ precursor ions are 1132, 815, 806, and 728 Da, respectively. The abundance-weighted average masses of z ions formed from these charge states are 1103, 682, 659, and 428 Da, respectively. Thus, the observed fragment ions shift toward lower mass with increasing precursor ion charge state.

The ECD fragmentation efficiency increases from 54 to 88% as the precursor charge state is increased from $(M + 2H)^{2+}$ to $(M + 5H)^{5+}$ (Table 1). ECD of the $(M + 2H)^{2+}$ was performed three times during a one-week period under the same set of conditions to assess the reproducibility of ECD spectra. The error (± one standard deviation from the mean) of the fragmentation efficiency of the $(M + 2H)^{2+}$ for three replicate measurements is ±10% (absolute). The fragmentation efficiencies calculated without $C_6H_{13}N_2O^+$ range from 52 ± 8 to 63%. The fragmentation efficiencies calculated without $C_6H_{13}N_2O^+$ are included as a more accurate measure of the efficiency with which structurally informative fragment ions are produced from a given precursor charge state (Table 1). The residual precursor ion decreases in abundance from 41 ± 12 to 10% TIA as the precursor ion charge state is increased from $(M + 2H)^{2+}$ to $(M + 5H)^{5+}$. Theoretical residual precursor ion abundances were calculated based on the quadratic dependence of the electron capture cross section on charge state.[23] The theoretical precursor ion abundances calculated for the $(M + 3H)^{3+}$, $(M + 4H)^{4+}$, and $(M + 5H)^{5+}$, normalized to the experimentally observed precursor ion abundance of the $(M + 2H)^{2+}$, are lower than the experimentally observed values by 15, 14, and 3% (absolute), respectively (Table 1). Possible reasons for not realizing the theoretical electron capture efficiency are incomplete overlap between the electron and ion clouds and the possible presence of fragment ions with abundances or *m*/*z* below the detection limits. In addition, slight discrepancies between the measured and the actual fragmentation and electron capture

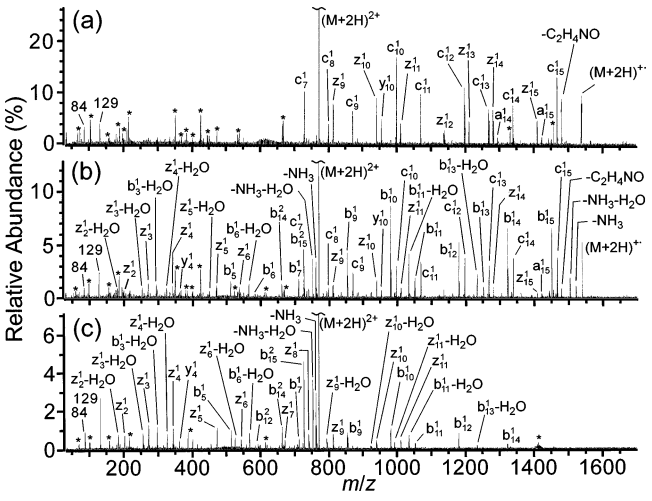

Figure 4. Spectra of the $(M + 2H)^{2+}$ collected at (a) 100 °C with ECD, (b) 150 °C with ECD, and (c) 150 °C without ECD. The peaks at *m/z* 129 and 84 are $C_6H_{13}N_2O^+$ and $C_4H_6NO^+$, respectively. Noise peaks are indicated by asterisks (the heating circuit used for the heated cell experiments results in spurious noise peaks).

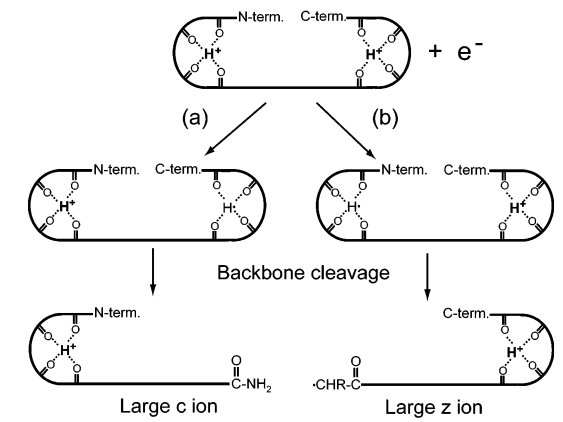

Figure 5. Mechanism for ECD of the $(M + 2H)^{2+}$. The charges (protonated lysine side chains) are located near the termini of the peptide and are solvated by backbone carbonyl oxygens. Electron capture and neutralization of the charge near the C-terminus (a) results in formation of a high-mass c ion and a low-mass, neutral z product. Similarly, neutralization of the charge near the N-terminus (b) produces a high-mass z ion and a low-mass, neutral c product. (The neutral products are not shown.)

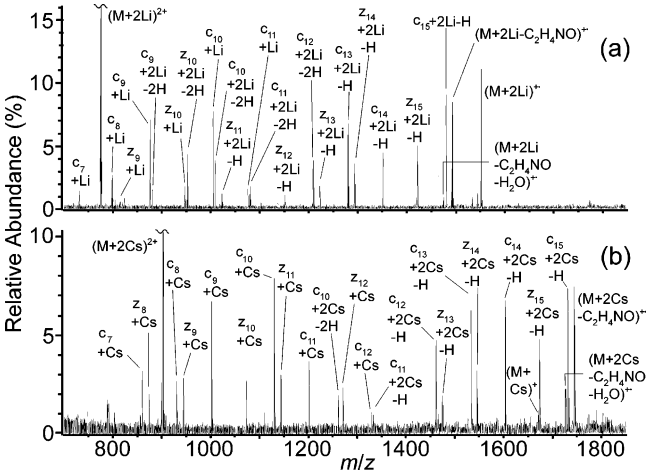

Figure 6. ECD spectra of the (a) $(M + 2Li)^{2+}$ and (b) $(M + 2Cs)^{2+}$.

efficiencies are introduced by the charge- and mass-dependent sensitivity of the ion cyclotron resonance signal.[34] Despite these uncertainties, it is clear that the ECD process can be very efficient.

ECD with Heated Cell. To determine whether the formation of exclusively large c and z ions from the $(M + 2H)^{2+}$ is due to tertiary structure, ECD was done with the ion cell temperature as high as 150 °C. The ECD spectrum is unchanged up to 100 °C (Figure 4a). At 150 °C, several new ions appear, including a wide range of b and z ions, b and z ions that have lost water, and residual precursor ion and reduced precursor ion that have lost water, ammonia, or both (Figure 4b). *No new c ions are formed by heating to 150 °C.* Although z ions have the same masses as the corresponding y ions that have lost ammonia, the c ions have masses that are different from those of the other fragment ions and, therefore, are diagnostic for backbone cleavage resulting from ECD.

To determine which of the ions in Figure 4b are products of blackbody infrared radiative dissociation[14,15] of the $(M + 2H)^{2+}$ at 150 °C, the experiment was repeated without injecting electrons into the cell; i.e., the ions were activated only by blackbody radiation. Like Figure 4b, the resulting spectrum in Figure 4c contains b, y, and z ions, neutral losses from b and z ions, and neutral losses from the precursor ion, but it does not contain c ions. The persistence of the limited range of observed c ions up to 150 °C indicates that tertiary structure is not the cause of the limited fragmentation observed for the $(M + 2H)^{2+}$ or that any tertiary or secondary structure is stable at this high temperature.

A more likely explanation for the formation of exclusively large c and z ions from the $(M + 2H)^{2+}$ is that backbone cleavages occur near charges.[20,35] In this mechanism, one lysine side chain near each peptide terminus is protonated, and the charges are solvated by polar groups of the local peptide backbone (Figure 5). Capture of an electron by the charge at the C-terminus results in the formation of a radical and subsequent cleavage nearby, resulting in a relatively large c ion and a small, neutral z fragment. Similarly, if the electron neutralizes the charge near the N-terminus, cleavage of the backbone results in a large z ion and a small, neutral c fragment. Additional charges will be located nearer the center of the sequence to minimize Coulombic repulsion, and thus will give rise to backbone cleavages closer to the middle of the sequence and hence smaller c and z ions, consistent with our observations (Figures 2 and 3).

ECD of Metalated Dications. ECD of the $(M + 2Li)^{2+}$ and $(M + 2Cs)^{2+}$ produces the lithiated and cesiated analogues of the same range of c and z ions formed from the $(M + 2H)^{2+}$, with the addition of cesiated z_8 formed from ECD of the $(M + 2Cs)^{2+}$. As shown in the ECD spectra of Figure 6 and the fragment ion plots of Figure 7, each fragment ion contains one or two Li or Cs, with the fraction of fragment ions having two Li or Cs increasing with fragment ion mass. For example, the c_7, c_8, and z_9 formed from the $(M + 2Li)^{2+}$ are exclusively monolithiated, while c_{12}–c_{15} and z_{12}–z_{15} are exclusively dilithiated (Figure 7a). Similarly, for ECD of the $(M + 2Cs)^{2+}$, c_7–c_9 and z_8–z_{12} are exclusively monocesiated and c_{13}–c_{15} and z_{13}–z_{15} are exclusively dicesiated

(34) Marshall, A. G.; Hendrickson, C. L.; Jackson, G. S. *Mass Spectrom. Rev.* **1998**, *17*, 1–35.

(35) Cerda, B. A.; Breuker, K.; Horn, D. M.; McLafferty, F. W. *J. Am. Soc. Mass Spectrom.* **2001**, *12*, 565–570.

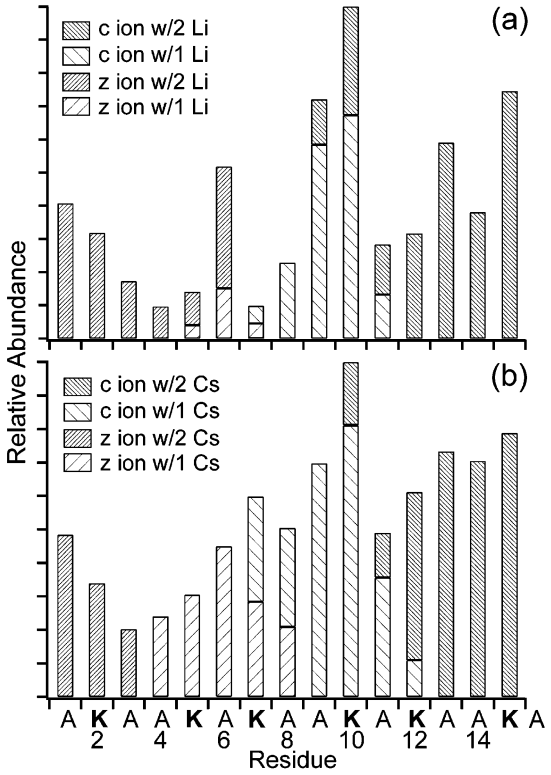

Figure 7. ECD fragment ion plots of the (a) $(M + 2Li)^{2+}$ and (b) $(M + 2Cs)^{2+}$.

(Figure 7b). The increasing fraction of dimetalated fragment ions with increasing ion mass is consistent with the metal cations being located near the termini of the peptide (Figure 7).

In the ECD spectrum of the $(M + 2Li)^{2+}$, the combined abundance of dilithiated c and z ions exceeds that of the monolithiated ions by 116% (Figure 7a). In contrast, for the $(M + 2Cs)^{2+}$, the combined abundance of dicesiated c and z ions is only 0.2% greater than that of the monocesiated ions (Figure 7b). The higher proportion of dimetalated fragment ions formed from the $(M + 2Li)^{2+}$ may be related to the differences in strength with which Li^+ and Cs^+ bind to the peptide backbone. In solution, the charge-shielding properties of the solvent enable two cations to approach each other more closely than they would in the gas phase. During desolvation of the $(M + 2Li)^{2+}$, the binding of the two lithium cations to the backbone is strong relative to the Coulombic repulsion between them, causing them to be "locked" into position. However, in the case of the $(M + 2Cs)^{2+}$, the cesium cations can more easily move away from each other during desolvation to minimize Coulombic repulsion since cesium is more weakly bound. Thus, in the gas-phase peptide dications, the more weakly bound cation, Cs^+, may be more likely to be located at the termini than the more strongly bound cation, Li^+. Results demonstrating that Cs^+ is not strongly bound and is "mobile" when the peptide is thermally activated are presented below.

ECD of Mixed Dications. The $(M + Cs + Li)^{2+}$ and $(M + H + Li)^{2+}$ were fragmented by ECD (Figures 8 and 9). ECD of the $(M + Cs + Li)^{2+}$ produces lithiated, cesiated, and mixed alkali analogues of the same c (c_7-c_{15}) and z (z_9-z_{15}) ions formed from the $(M + 2H)^{2+}$ (Figures 8a and 9a). As also observed with the $(M + 2Li)^{2+}$ and $(M + 2Cs)^{2+}$, the abundance ratio of dimetalated

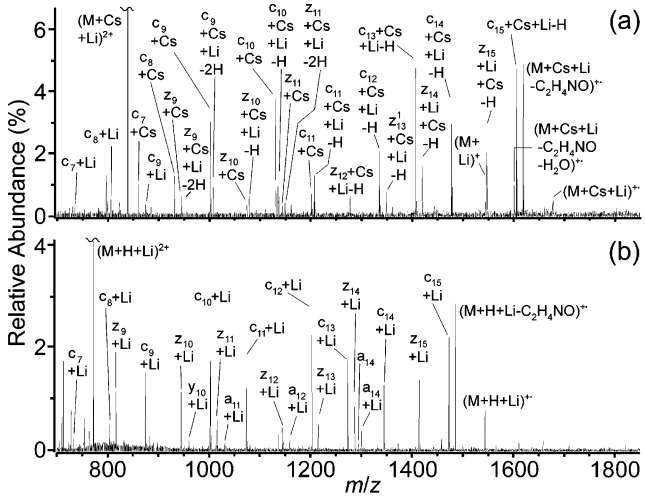

Figure 8. ECD spectra of the (a) $(M + Cs + Li)^{2+}$ and (b) $(M + H + Li)^{2+}$.

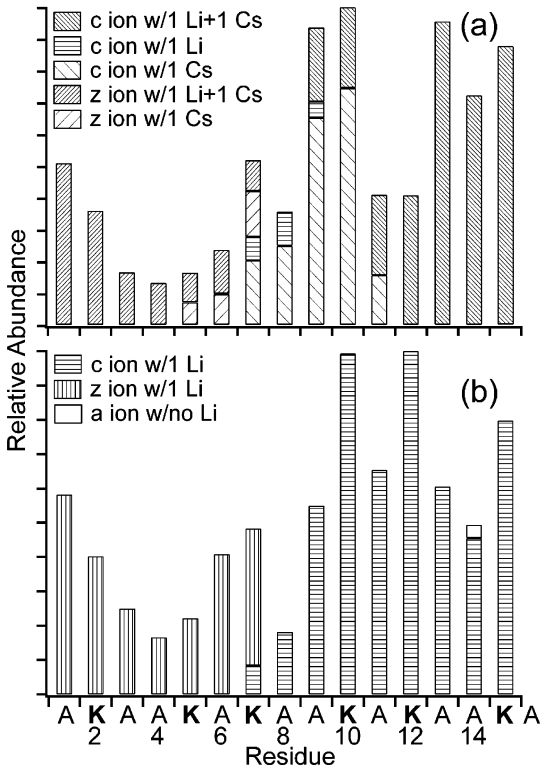

Figure 9. ECD fragment ion plots of the (a) $(M + Cs + Li)^{2+}$ and (b) $(M + H + Li)^{2+}$.

to monometalated fragment ions increases with increasing fragment ion mass. Monolithiated c_7-c_9 and monocesiated c_7-c_{11} and z_9-z_{11} are observed. The $c_{12}-c_{15}$ and $z_{12}-z_{15}$ analogues have both Li and Cs (Figure 9a). No z ions containing only Li are detected. The abundance ratio of cesiated fragment ions to lithiated fragment ions is 10:1, indicating a preference for Cs^+ to remain charged and Li^+ to be neutralized during ECD.

Interestingly, ECD of the $(M + H + Li)^{2+}$ results in exclusively lithiated analogues of c_7-c_{15} and z_9-z_{15} (Figures 8b and 9b). The only protonated fragment ion observed is the a_{14}, constituting 0.5% of the total fragment ion abundance. The abundance ratio for lithiated to protonated fragment ions is 200:1, suggesting an

Table 2. Calculation of the Recombination Energy of Protonated, Lithiated, and Cesiated Glycine

cationizing agent	ionization energy of neutral atom (kcal/mol)[a]	cation affinity (kcal/mol)[b]	neutral atom affinity (kcal/mol)	recombination energy (kcal/mol)
H^+	314	212	14[c]	116
Li^+	124	51	12[d]	85
Cs^+	90	21	~3[e]	72

[a] From ref 36. [b] The H^+, Li^+, and Cs^+ affinities of glycine, from refs 37−39, respectively. [c] The H atom affinity of a carbonyl group (ref 40). [d] The Li atom affinity of acetone (ref 41). [e] The Cs atom affinity of acetone (estimated).

overwhelming preference for Li^+ to remain charged and H^+ to be neutralized during ECD.

The recombination energy (RE)[21] is a measure of the thermodynamic favorability of electron capture at a protonated or metal-cationized site. The RE of a species, e.g., a peptide ion, with n elementary positive charges can be estimated from eq 1,

$$RE = IE - CA + NA \quad (1)$$

where IE is the ionization energy of the neutral atom (H, Li, or Cs), CA is the cation (H^+, Li^+, or Cs^+) affinity of the species with $n - 1$ charges, and NA is the neutral atom (H, Li, or Cs) affinity of the species with $n - 1$ charges.

To obtain a rough estimate of the relative RE values for molecules with H^+, Li^+, and Cs^+ attached, these values for glycine were estimated. Values of the IEs of H, Li, and Cs atoms,[36] and the H^+, Li^+, and Cs^+ affinities of glycine,[37−39] are available, but values of NA of glycine are not. The H atom affinity of a carbonyl group[40] and the lithium atom affinity of acetone[41] are used as approximate NA values in this calculation. The Cs atom affinity of acetone, which has not been published, is estimated as ~3 kcal/mol based on the known H, Li, and Na atom affinities (14,[40] 12,[41] and 7 kcal/mol,[41,42] respectively).

The estimated RE values for protonated, lithiated, and cesiated glycine based on the approximation described above are 116, 85, and 72 kcal/mol, respectively (Table 2). Of course the RE values of the peptide ions will differ from those of protonated/cationized glycine, due to the presence of multiple polar backbone groups and charges in the former. Nonetheless, the RE values of glycine with the various cations may be a useful measure of the relative RE values of the cationized peptide. The estimated RE of lithiated glycine exceeds that of cesiated glycine by 13 kcal/mol, consistent with the preferred neutralization of Li^+ over Cs^+ observed in ECD

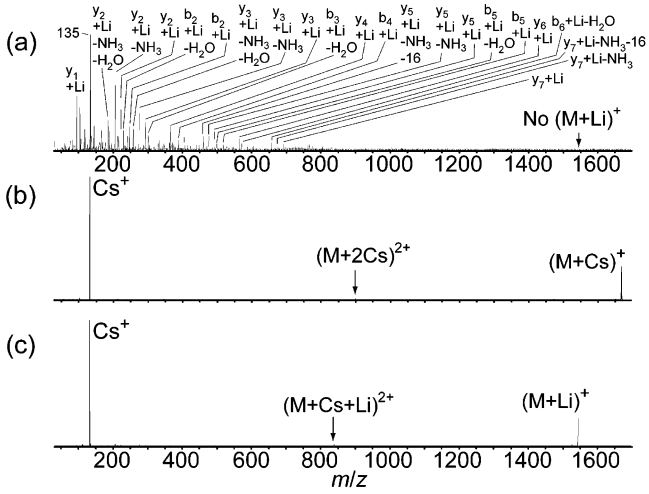

Figure 10. SORI-CAD spectra of the (a) $(M + 2Li)^{2+}$, (b) $(M + 2Cs)^{2+}$, and (c) $(M + Cs + Li)^{2+}$. The peak at *m/z* 135 in (a) is $LiC_6H_{12}N_2O^+$.

of the $(M + Li + Cs)^{2+}$. Similarly, the estimated RE of protonated glycine exceeds that of lithiated glycine by 31 kcal/mol, consistent with the overwhelming preference for neutralization of H^+ over Li^+ in ECD of the $(M + Li + H)^{2+}$. The difference between the RE values of protonated and lithiated glycine is 2.4 times as great as the difference between those of lithiated and cesiated glycine. This is consistent with the greater preference observed for neutralization of H^+ over Li^+ in ECD of the $(M + Li + H)^{2+}$ (200-fold) than for neutralization of Li^+ over Cs^+ in the $(M + Li + Cs)^{2+}$ (10-fold).

Collisionally Activated Dissociation. The $(M + 2Li)^{2+}$, $(M + 2Cs)^{2+}$, and $(M + Cs + Li)^{2+}$ were activated by SORI-CAD (Figure 10). Activation of the $(M + 2Li)^{2+}$ results in several lithiated b and y ions, lithiated b and y ions that have lost ammonia, water, or both, and $LiC_6H_{12}N_2O^+$ (*m/z* 135). The latter ion is the lithiated analogue of the protonated internal cleavage product, $C_6H_{13}N_2O^+$ (*m/z* 129), formed from protonated 6KI ions (Figure 2). Lithium ion ejection to form $(M + Li)^+$ (*m/z* 1545) does not occur (Figure 10a). In contrast, the SORI-CAD spectra of the $(M + 2Cs)^{2+}$ and $(M + Cs + Li)^{2+}$ are dominated by the products of Cs^+ ejection, with Cs^+ as the base peak in both spectra and $(M + Cs)^+$ and $(M + Li)^+$ observed at 27 and 22% relative abundance, respectively (Figure 10b and c). These results are consistent with Cs^+ being more weakly bound to the peptide backbone than Li^+, consistent with its much larger radius (the radii of Cs^+ and Li^+ are 1.9 and 0.76 Å, respectively).[36] This is yet another demonstration of the novel ability of ECD to cleave peptide backbone bonds without ejecting labile species.

CONCLUSIONS

ECD and CAD of a lysine- and alanine-containing peptide cationized with different combinations of H^+, Li^+, and Cs^+ were investigated. ECD of the $(M + 2H)^{2+}$ produces only large c and z fragment ions, but ECD of higher charge states produces both large and small fragment ions, with a shift toward lower mass fragment ions with increasing charge state. Heating the $(M + 2H)^{2+}$ to 150 °C during ECD does not increase the range of fragment ions formed by ECD, indicating that the limited range of product ions formed from this charge state is not due to effects

(36) Lide, D. R., Ed. *CRC Handbook of Chemistry and Physics*; CRC Press: Boca Raton, FL, 1996.
(37) Hunter, E. P.; Lias, S. G. In *NIST Chemistry Webbook*, NIST Standard Reference Database 69; Mallard, W. G., Lindstrom, P. J., Eds.; National Institute of Standards and Technology: Gaithersburg, MD 29899, March 1998.
(38) Bojesen, G.; Breindahl, T.; Andersen, U. N. *Org. Mass Spectrom.* **1993**, *28*, 1448−1452.
(39) Hoyau, S.; Ohanessian, G. *Chem. Eur. J.* **1998**, *4*, 1561−1569.
(40) Zubarev, R. A. *Mass Spectrom. Rev.* **2003**, *22*, 57−77.
(41) Tsunoyama, H.; Ohshimo, K.; Yamakita, Y.; Misaizu, F.; Ohno, K. *Chem. Phys. Lett.* **2000**, *316*, 442−448.
(42) Wang, L.-T.; Su, T.-M. *J. Phys. Chem. A* **2000**, *104*, 10825−10833.

of tertiary structure. This phenomenon is more likely a result of backbone cleavages occurring near the neutralized charges. ECD of the $(M + 2Li)^{2+}$ and the $(M + 2Cs)^{2+}$ produces mono- and dimetalated analogues of the fragment ions formed from the $(M + 2H)^{2+}$, with the proportion of dimetalated to monometalated fragment ions increasing with fragment ion mass. In contrast, collisional activation of the $(M + 2Li)^{2+}$ and $(M + 2Cs)^{2+}$ produces markedly different spectra, with the products of backbone cleavage and neutral losses dominating the former and products of Cs^+ ejection dominating the latter. The abundance of cesiated fragment ions exceeds that of lithiated fragment ions in the ECD spectrum of the $(M + Cs + Li)^{2+}$ by 10:1, and all c and z ions formed from ECD of the $(M + H + Li)^{2+}$ are lithiated. These results are consistent with the preferred neutralization of the cation of highest recombination energy.

ACKNOWLEDGMENT

The authors acknowledge Dr. David King (UC Berkeley) for synthesizing the peptide used in this study. Generous financial support for this research was provided by the National Institutes of Health (Grant R01-GM64712-01).

Received for review December 4, 2003. Accepted February 10, 2004.

AC035431P